ELSEVIER

Journal of Nuclear Materials 317 (2003) 62–68

journal of nuclear materials

www.elsevier.com/locate/jnucmat

On the solubility of chromium sesquioxide in uranium dioxide fuel

A. Leenaers [a,*], L. de Tollenaere [b], Ch. Delafoy [c], S. Van den Berghe [a]

[a] *SCK • CEN, Reactor Materials Research, Boeretang 200, B-2400 Mol, Belgium*
[b] *FBFC International, Europalaan 12, B-2480 Dessel, Belgium*
[c] *FRAMATOME ANP, Rue Juliette Récamier 10, 69456 Lyon cedex 06, France*

Received 1 October 2002; accepted 10 December 2002

Abstract

Chromium sesquioxide doped uranium dioxide systems with a variety of initially added Cr_2O_3 amounts were prepared under different sintering conditions. The solubility limit of Cr for each sintering condition is derived from the measured content of the dopant dissolved in the UO_2 matrix using electron probe microanalysis (EPMA). It is found that the solubility of chromium in a uranium dioxide system for these series sintered at 1600, 1660 and 1760 °C is limited to respectively 0.065 ± 0.002, 0.086 ± 0.003 and 0.102 ± 0.004 wt% Cr. The lattice parameters of the different Cr_2O_3 doped fuels have been examined with X-ray diffraction (XRD). The XRD peaks of the samples sintered at 1760 °C as well as a UO_2 reference without Cr, prepared under the same conditions, were measured and a value for the lattice parameter *a* for each sample was obtained using the unit cell refinement method. A slight contraction of the lattice parameter is observed with increasing dopant content.

PACS: 28.41.Bm; 61.10.Nz; 61.72.Ss

1. Introduction

Currently the interest of the utilities and of the nuclear fuel vendors goes to improve in a significant way the in-pile performance of the UO_2 fuel intended for pressurized water reactors. The performance of the UO_2 fuel is limited today by two phenomena being the pellet–clad interaction, which reduces the reactor operation flexibility, and the fission gas release, which accelerates at high burnup. In order to gain margins on these two goals, advanced fuels are being developed. Amongst other possible options, the use of additives can influence the thermo-physical properties and improve fuel performance [1–3]. Several additives have been and are being considered (e.g. oxides of chromium [2–7], aluminium [3,8], vanadium [8], niobium [6,7,9], silicon [3], magnesium [3] and titanium [7–9]) because of their advantageous effect on one of the aforementioned phenomena occurring in the fuel. As shown by the studies carried out by CEA [5,8,10], Cr_2O_3 is an effective grain growth promoter, provokes an improvement of the creep properties of UO_2 (higher plasticity) and is expected to lead to a better retention of the fission gases.

All the above mentioned properties depend on the amount of additives dissolved in the fuel matrix, which in turn depends on the sintering conditions. Suitable sintering atmospheres and resulting solubility limits have been studied for several dopants [5–8,11]. The solubility limits of other elements, especially fission products in UO_2 have also been determined [12,13].

However, the determination of the solubility limits of the dopants (chromium, aluminium, vanadium and titanium sesquioxides) in the experiments of Bourgeois

* Corresponding author. Tel.: +32-14 333044; fax: +32-14 321216.
E-mail address: aleenaer@sckcen.be (A. Leenaers).

0022-3115/03/$ - see front matter
doi:10.1016/S0022-3115(02)01693-8

et al. [8,5] are based mainly on the study of the variations in grain size as a function of the initial dopant concentration. It is assumed that grain growth is inhibited by the presence of precipitates that develop when the solubility limit is exceeded, because they anchor the grain boundaries. On this basis, a solubility limit of 0.07 wt% Cr_2O_3 (0.048 wt% Cr) in UO_2 sintered in a H_2–1vol.%H_2O atmosphere at 1700 °C (oxygen potential $\mu(O_2) = -430$ kJ/mol) was proposed.

In a study on the possible chemical interactions between uranium dioxide fuel and the austenitic steel fuel pin cladding at high temperature, Kleykamp [13] derived the maximum solubility limit of several steel components in the UO_{2-x} matrix after different heat treatments using electron probe microanalysis (EPMA). It was found that the maximum solubility of chromium in UO_{2-x} is 0.22 mol% Cr (0.128 wt% Cr) at 1500 °C and 0.32 mol% Cr (0.186 wt% Cr) at 2000 °C.

In the current study, the solubility limit of chromium sesquioxide in uranium dioxide is also derived from direct measurements of the actual content of the dopant dissolved in the UO_2 matrix. It is determined by EPMA for a variety of samples with different initially added amounts of Cr_2O_3 which were prepared under different sintering conditions. In addition, the solution type (interstitial or substitutional solid solution) of the Cr_2O_3-UO_2 solid solution is examined. The diffraction patterns of some samples sintered at 1760 °C were recorded by X-ray diffraction (XRD) analysis and their lattice parameters were refined on the basis of these patterns.

2. Experimental

2.1. Sample preparation

Commercial UO_2 powder, obtained by a dry process, was mixed with weighted amounts of Cr_2O_3 powder, in concentrations varying from 0.125 to 0.225 wt% Cr_2O_3 (0.0855–0.1540 wt% added Cr).

The powder mixture was pressed into pellets and subsequently sintered under different conditions. During the sintering process, the dewpoint of the atmosphere was controlled to fix the oxygen potential ($\mu(O_2)$). At temperature T, a theoretical value of $\mu(O_2)$ can be calculated from the dew point or the water-to-hydrogen ratio p_{H_2O}/p_{H_2}, through [14]:

$$RT\ln p_{O_2} = -479\,070 + 4.18T\left[8.86\log T - 4.42 + 9.152\log\left(\frac{p_{H_2O}}{p_{H_2}}\right)\right] \quad (\mathrm{J/mol\ O_2}). \qquad (1)$$

One batch of samples has been sintered at 1760 °C. The measured dew point corresponds to an oxygen potential of around −390 kJ/mol O_2. The second series was sintered at the same temperature but in an atmosphere with a higher dew point ($\mu(O_2) \approx -360$ kJ/mol O_2). The third and fourth batch were both sintered at respectively 1660 and 1600 °C with $\mu(O_2) \approx -370$ kJ/mol O_2. The samples and sintering conditions are summarised in Table 1. During cooling down, the atmosphere is switched back to dry hydrogen when the temperature drops below about 1000 °C.

Table 1
Definition of samples and preparation conditions

Sintering temperature (°C)			
1760	1760	1660	1600
Oxygen potential ($\mu(O_2)$) (kJ/mol O_2))			
−390	−360	−370	−370
Initially added wt% Cr ($wt\%\ Cr_2O_3$)			
0.1025 (0.150)	0.0855 (0.125)	0.1025 (0.150)	0.1025 (0.150)
0.1200 (0.175)	0.1200 (0.175)	0.1200 (0.175)	0.1200 (0.175)
0.1365 (0.200)	0.1540 (0.225)	0.1365 (0.200)	0.1365 (0.200)

2.2. Electron probe microanalysis

The pellets have been embedded in epoxy resin and polished with SiC paper of successively finer grain size, finishing on cloth with diamond paste of 3 and 1 μm. Before mounting the sample in the electron microscope, the samples were coated with carbon to prevent charging. The EPMA is performed in a shielded CAMEBAX-R Microbeam, upgraded with digital image and X-ray acquisition programs (SAMx Suite).

The elemental composition of the pellets is measured by wavelength dispersive X-ray analysis. A PC1 (synthetic multilayer), LiF and PET crystal were selected to measure respectively OKα, CrKα and UMα. Prior to the measurement on each pellet, calibration is performed on a MOX standard (65.79 wt% U, 21.56 wt% Pu, 11.85 wt% O) and a pure chromium standard. To convert the measured intensities to concentrations, a $\varphi\rho z$ procedure is applied. The chromium, uranium and oxygen contents of the UO_2 matrix were determined from a line scan over the pellet diameter (80 analysed points), with a stepsize of approximately 100 μm. The electrons were focussed on a spot of $\leqslant 1$ μm to avoid chromium concentration spots (precipitates). The instrumental parameters have been optimised for quantification of chromium, resulting in a low detection limit within a reasonable measuring time (Table 2). For the analysis of precipitates, a lower acceleration voltage has been used to avoid the contribution of the surrounding matrix. This is also beneficial for the interpretation of oxygen concentration

Table 2
Minimum detection limit according to 3σ criterion

	Accelerating voltage (kV)	Beam current (nA)	Detection limit (wt %)		
			Cr	U	O
Matrix	20	100	0.003	0.024	0.009
Precipitates	10	100	0.030	0.030	0.005

measurements. For 10 precipitates, distributed evenly on the pellet diameter, the chromium, uranium and oxygen contents were measured.

2.3. X-ray diffraction

The lattice parameters of the samples sintered at 1760 °C ($\mu(O_2) = -360$ kJ/mol O_2) were determined by XRD. A Philips X'Pert θ–θ diffractometer equipped with a Cu tube ($CuK\alpha_{1,2} = 0.1541$ nm), was configured for standard powder diffraction measurements (Bragg–Brentano geometry). Scans of the various UO_2 diffraction peaks in the 20–140° 2θ range were recorded with the X'Celerator, an X-ray area detector based on real time multiple strip technology. The used stepsize is $2\theta = 0.00841°$, measuring a total of 30 s per step. To eliminate the CuKβ contribution, a nickel filter is used and to reduce the background, a small anti-scatter shield is mounted in front of the detector.

For accurate measurements, important sources of error, such as goniometer zero shift and eccentricity of the incident beam with respect to the goniometer axis, have to be eliminated by careful system alignment. To eliminate further systematic errors an external standard reference (NIST Standard Reference Material 660a: $LaB_{6,}$) is measured [15]. Although this standard is mainly intended for peak profile analysis, it comes with a certified lattice parameter ($a = 0.41569162 \pm 0.00000097$ nm), determined by the NIST.

The peak positions of the standard phase are compared to their theoretical values and a correction curve (polynomial) is calculated, which describes the aberrations in 2θ [16]. This correction curve is used to eliminate systematic errors in the actual measurements. Lastly the sample displacement is calculated and corrected for. All corrections were found to be very small.

To deduce the cell parameters from a measurement, a unit cell refinement [16] is used.

The Smith–Snyder figure of merit (FOM) gives an objective quantitative estimate of the quality of the metric aspects of a powder pattern (i.e. the location of the diffraction peaks and not their heights). FOMs above 80 are considered high quality, and those less than 20 are rather poor quality [15].

The measurement and refinement methods described above do not guarantee a correct determination of the absolute values for the lattice parameter a, but it does provide a sound basis to compare the lattice parameter values of the different samples.

3. Results

3.1. Solubility limits

A typical result of a quantitative diameter line scan of a Cr_2O_3 doped UO_2 pellet is presented in Fig. 1 by means of a line plot, showing the measured wt% of U,

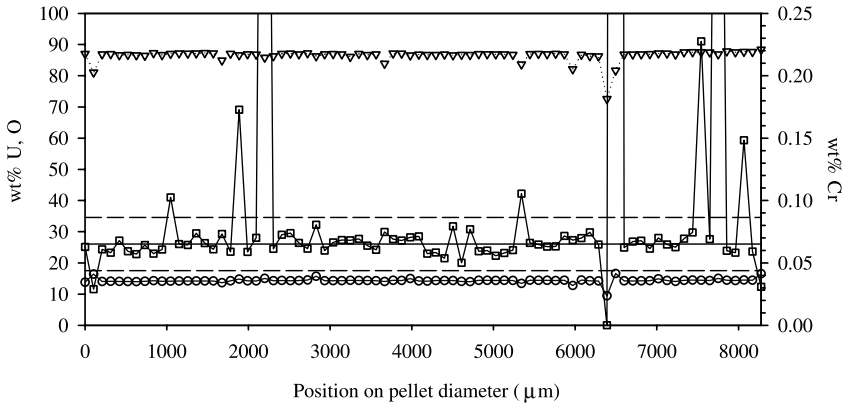

Fig. 1. Results of a typical pellet diameter scan of the uranium (∇), oxygen (O) and chromium (□) contents (wt%). The solid line represents the mean Cr content, the dashed lines show the statistical error ($\pm 2\sigma$).

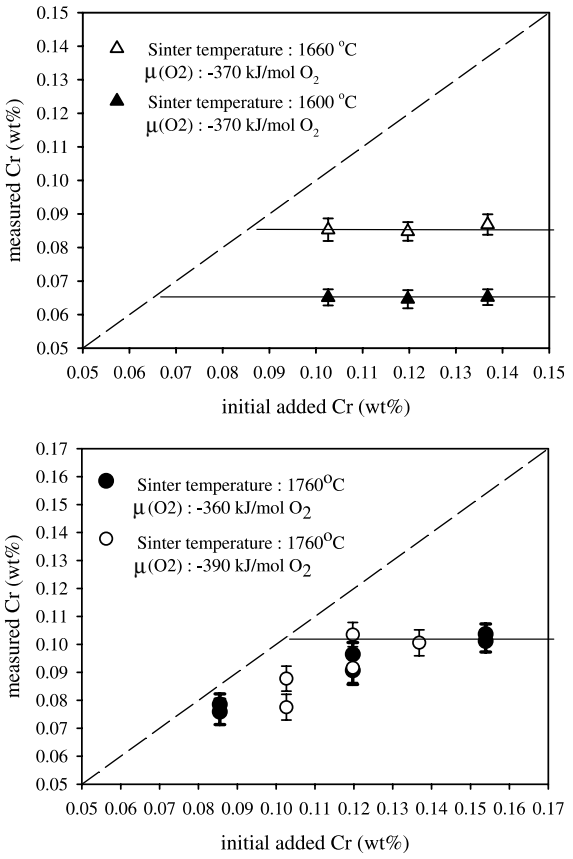

Fig. 2. Measured Cr-contents in the UO_2 matrix sintered at different temperatures (a,b) as a function of initial added chromium enrichment. The solid line represents the solubility limit, the dashed line the maximum possible dissolved chromium content.

O and Cr as function of the position on the pellet diameter.

The combined weight percentage of the three elements should amount to a total of 100%. Due to systematic errors, this value can deviate by about 10% absolute, but the relative error is lower than 2%. The occasional higher values for Cr are due to the contribution of (sub)surface chromium precipitates, while the simultaneous low values for U, O and Cr indicate the presence of pores. The mean Cr concentration in the matrix of each pellet has been calculated excluding the measurements on pores and precipitates. In Fig. 2 the mean Cr contents for all pellets in each series are plotted against the initially added Cr_2O_3 contents, converted to the initially added Cr amount.

The samples of the series sintered at 1600 and 1660 °C show almost no variation in the chromium content of the matrix with different initial chromium enrichments. On the condition that an equilibrium was established during sintering, this means that for these series, the solubility limit can be determined to be respectively 0.065 ± 0.002 and 0.086 ± 0.003 wt% Cr. Further enrichment of the initial blend will not introduce more chromium in the matrix but rather induce precipitation. For the series of samples sintered at 1760 °C, such a saturation of the matrix is observed at initial enrichments of 0.120 wt% Cr (0.175 wt% Cr_2O_3) or higher. Before saturation, the measured Cr concentrations are not exactly equal to the initially added amounts, because some chromium is lost during sintering by evaporation and some small chromium concentration spots are still present. The measured Cr content leads to a solubility limit of 0.102 ± 0.004 wt% Cr for this series.

3.2. Precipitates

In all of the samples, small precipitates ($\simeq$3 μm) are observed, although not in large amounts. For all series, the composition of the precipitates is found to be very close to Cr_2O_3 (Fig. 3(a)), except for the series sintered at 1760 °C at an oxygen potential of −390 kJ/mol O_2, where the composition of some of the precipitates is near to 'CrO' (Fig. 3(b)). Although CrO is not a stable phase,

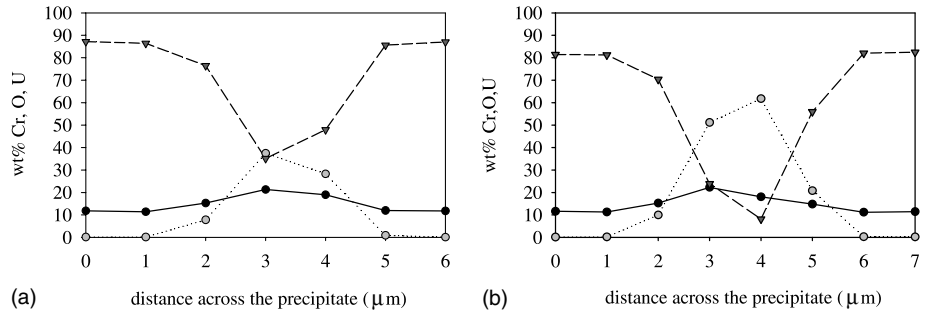

Fig. 3. Measured chromium (dotted line), uranium (dashed line) and oxygen (solid line) content by EPMA of some precipitates found in the sample sintered at 1760 °C ($\mu(O_2) = -390$ kJ/mol). Quantitative analysis identifies (a) as a Cr_2O_3 while for (b) the composition is closer to CrO.

the stoichiometry of these precipitates indicates that some reduction of the Cr_2O_3 has taken place.

3.3. Lattice parameters

The crystal structure of UO_2 is of the fluorite type. Since this is a cubic structure, only one lattice parameter (a) has to be measured to characterise the unit cell dimensions. The XRD peaks of the samples sintered at 1760 °C ($\mu(O_2) = -360$ kJ/mol O_2) as well as a UO_2 reference without Cr, prepared under the same conditions were measured, and a value for the lattice parameter a for each sample was obtained using the unit cell refinement method. From the diffraction pattern in Fig. 4 it can be seen that there is a shift in the peak position of the sample containing 0.1012 wt% Cr to a higher 2θ value (or smaller d value), compared to the peak positions of the pure UO_2 standard. This indicates that the lattice parameter a for the 0.1012 wt% Cr sample will be smaller than the lattice constant of UO_2.

Before refining the cell parameters of the samples, the measurements are corrected for systematic and zero shift errors as described above. For all the measured and refined diffraction patterns, the Smith–Snyder FOM ranges between 185 and 290 indicating the good quality of the refinement. The resulting lattice parameters found are summarized in Table 3.

As stated earlier, one should focus on the relative values rather than on the absolute lattice parameters.

The found lattice parameters of Cr_2O_3 doped UO_2 (1760 °C, −360 kJ/mol O_2) with varying Cr contents, are plotted in Fig. 5 against the measured Cr contents.

The lattice parameter a of the samples sintered at 1600 and 1660 °C, the series where the solubility limit had been reached, have also been measured. Within a series, as expected, all the samples gave the same lattice parameter. However, the diffraction patterns measured in both series, showed broad peak profiles. For the diffraction peaks of the samples sintered at 1600 and 1660 °C a full width at half maximum (FWHM) of $2\theta = 0.13°$ and 0.1° respectively, have been found, in contrast to a FWHM of $2\theta = 0.07°$ for the diffraction peaks of the series sintered at 1760 °C and the UO_2 standard. The large FWHM found for these series could indicate that the samples are not fully sintered. As a result, the measured lattice parameters for both series, deviate from the lattice parameters found in the series sintered at 1760 °C and are not considered further.

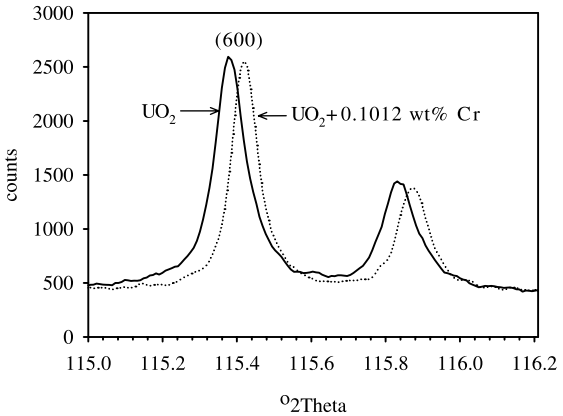

Fig. 4. The (6 0 0) $K\alpha_{1,2}$ doublet of the UO_2 standard (solid line) and of the sample containing $UO_2 + 0.1012$wt%Cr (dashed line).

Table 3
Lattice parameter a of pure and chromium sesquioxide doped uranium dioxide systems

Measured Cr content in wt% (σ)	Measured lattice parameter a in nm (σ)
0	0.547065(3)
0.0785(38)	0.547014(3)
0.0907(50)	0.547009(5)
0.0964(42)	0.547002(5)
0.1012(39)	0.546994(5)

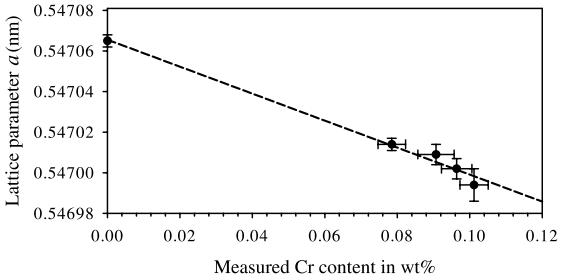

Fig. 5. Obtained lattice parameter a as a function of measured chromium content by EPMA. The dashed line represents a linear regression analysis.

4. Discussion

From the EPMA results, the solubility limit for the various chromium sesquioxide doped uranium dioxide samples with different initially added Cr_2O_3 concentrations, could be derived. It can be deduced that the solubility limit of the different series increases with temperature (Fig. 6), as is generally expected for dissolution. In principle, the solubility of a dopant in a UO_2 matrix depends on the oxygen potential and temperature. In this study, due to the small variation in oxygen potential during sintering, the observed increase in solubility limit of the different series has to be attributed primarily to temperature and not to oxygen potential differences.

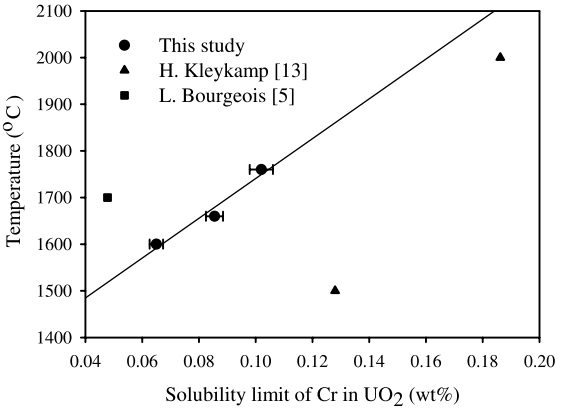

Fig. 6. Solubility limit of Cr in UO_2 matrix as a function of the applied sintering temperature. The solid line represents a linear regression analysis on the data point found in this study, but is merely intended to guide the eye and not as an extrapolation of our data.

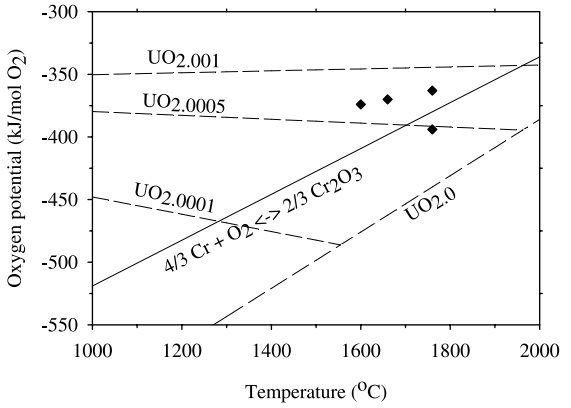

Fig. 7. Oxygen potential vs. temperature diagram indicating the equilibrium Cr/Cr_2O_3 and the oxygen potential of $UO_{2.0}$ and UO_{2+x} for various x, according to Lindemer and Besman [11]. The inserted points position the sinter atmospheres of the current experiments.

The solubility limits of metallic chromium in UO_{2-x} derived by Kleykamp [13], are higher compared to the results found in this study (Fig. 6). This difference can be attributed to the fact that the stoichiometry of the uranium dioxide matrix is different, as well as to the difference in the heat treatments of the samples.

In all the samples of the different series, several small precipitates could be found, even if the solubility limit had not been reached. If the solubilisation of chromium oxide in the UO_2 matrix has slow kinetics, these observed precipitates might be the remnants of the initial powder particles that have not been completely dissolved. The majority of the precipitates consists of Cr_2O_3. The calculation of the oxygen potential of the sinter atmosphere [17], allows us to position the oxygen potential during sintering in an Ellingham diagram (Fig. 7). It is found that the oxygen potentials of the atmospheres for the different series do not differ that much, but one can see that for the batch sintered at 1760 °C, $\mu(O_2) = -390$ kJ/mol O_2, the sintering takes place below the Cr/Cr_2O_3 equilibrium, where a reduction of Cr_2O_3 is possible [18].

This can explain the existence of the 'CrO' precipitates in the series sintered at 1760 °C at an oxygen potential of −390 kJ/mol. These sintering conditions are consistent with the domain of existence of the CrO compound as presented by Toker [19] in a thermo-dynamic study of the Cr–O system. However, it should be noted that the industrial production method applied for the sample production, requires different $\mu(O_2)$ regimes during the various sintering steps (temperature rise, sintering, cooling) and therefore does not allow a precise definition of the $\mu(O_2)$ during the complete process.

XRD measurements show that the lattice parameter decreases with increasing dopant concentration. From literature [20], it was found that for various cation doped solid solutions, the lattice parameters vary linearly with the dopant concentration, only in the region where complete solid solutions are established. This is in accordance with Vegard's law [21], which states that the lattice parameters of the solid solutions change linearly with the composition.

In literature it is suggested that Cr^{3+} ions enter CaF_2 in substitution [22]. This is derived from electron paramagnetic resonance measurements, which suggest a trigonal symmetry with Cr^{3+} ions in a cation substitutional position. As CaF_2 is the isomorphic structure of UO_2, one could assume a similar substitution when doping UO_2 with Cr^{3+} ions. However, one has to take into account that the substitution of a Ca^{2+} ion with a Cr^{3+} ion is different from substituting a U^{4+} ion with Cr^{3+}. It is known for metals that the solubility is higher if the solute (Cr^{3+}) has a higher valence than the solvent (Hume–Rothery rules). In parallel, the Cr^{3+} environment of F^- ions is different from an O^{2-} environment.

Although the substitution of a large U^{4+} ion with the small Cr^{3+} ion, would result in a decrease of the lattice parameter, as observed from the XRD measurements, the difference in relative size of the ions is too high. The ionic radii of Cr^{3+} and U^{4+} are respectively 61 and 114 pm [23] (remark: the ionic radius of Cr^{3+} is only known in a coordination 6), which results in a difference of 86%. According to the Hume–Rothery rules, substitution of U^{4+} ion with Cr^{3+} ion would create very large lattice distortions. These large distortions are expected to lead to large lattice parameter changes, even for low dopant concentrations, while the determined variations in a are small. Furthermore, the current XRD experiment shows that the resulting structure of Cr^{3+} doped UO_2 is still cubic and its diffraction lines show no indication of

broadening. Both these findings are not in support of the Cr^{3+} ions entering the UO_2 matrix in substitution.

The ionic radius of Cr^{3+} is small enough to fit the 100 pm of the interstitial sites in the UO_2 lattice. This is also assumed for Ti^{3+} and Nb^{4+}, which have ionic radii of respectively 67 and 79 pm [4,6,7,9]. To balance the introduction of an interstitial trivalent element, the cation vacancies and/or the oxygen interstitials will increase, in turn leading to a subsequent oxidation of U^{4+} to U^{5+}. Although interstitial solid solutions lead to larger lattice parameters, the U^{5+} ionic radius is smaller than for U^{4+}, thus causing a decrease in a. The combination of these effects could cause the net effect of the observed decrease of the lattice parameter.

The assumption of a cationic interstitial solid solution would also be in compliance with the fact that the resulting increase of the concentration of cation vacancies and oxygen interstitials is expected to cause the increase of the cation diffusion coefficients of Cr_2O_3 doped UO_2. The enhanced cation diffusion eventually increases the creep and grain growth rates [9].

5. Conclusion

The solubility limit of chromium sesquioxide doped uranium dioxide systems with a variety of initially added Cr_2O_3, prepared under different sintering conditions, has been derived from direct measurement using EPMA. It was found that for the series sintered at 1600 °C ($\mu(O_2) = -370$ kJ/mol O_2), 1660 °C ($\mu(O_2) = -370$ kJ/mol O_2) and 1760 °C ($\mu(O_2) = -360$ kJ/mol O_2, $\mu(O_2) = -390$ kJ/mol O_2) the solubility of chromium in a uranium dioxide system is limited to respectively 0.065 ± 0.002, 0.086 ± 0.003 and 0.102 ± 0.004 wt% Cr.

Characterization of the effects on the crystal structure related to the introduction of chromium sesquioxide in uranium dioxide for pellets sintered at 1760 °C ($\mu(O_2) = -360$ kJ/mol O_2), shows a slight decrease of the lattice parameter with increasing dopant concentration. From the linearity of the data points (within the error limits), it can be concluded that the samples in this series are true solid solutions.

Whether it concerns a substitutional or interstitial solid solution cannot be deduced conclusively from the current experiment. Simply based on differences in ionic radii, a substitutional solution would result in a decrease of lattice parameter, but would give rise to strongly distorted lattices. An interstitial solution would be more favoured, based on the fact that Cr^{3+} is small enough to fit the interstitial sites in the UO_2 lattice. The decrease of the lattice parameter a is explained by the resulting increase of the cation vacancies and/or the oxygen interstitials accompanied by an oxidation of U^{4+} to the smaller ion U^{5+}.

References

[1] Ph. Dehaudt, C. Lemaignan, L. Caillot, A. Mocellin, G. Eminet, Technical Committee Meeting on Advances in Pellet Technology for Improved Performance at High Burnup, Tokyo, Japan, IAEA-TECDOC-1036, 1196.
[2] J.C. Killeen, J. Nucl. Mater. 88 (1980) 177.
[3] S. Kashibe, K. Une, J. Nucl. Mater. 254 (1998) 234.
[4] K. Winter, Kernenergie 8 (1965) 413.
[5] L. Bourgeois, Ph. Dehaudt, C. Lemaignan, A. Hammou, J. Nucl. Mater. 297 (2001) 313.
[6] K. Naito, T. Tsuji, T. Matsui, J. Radioanal. Nucl. Chem. 143 (1990) 221.
[7] K. Naito, T. Tsuji, T. Matsui, in: J. Nowomy, W. Weppner (Eds.), Non-Stoich. Compds. – Surfaces, Grain Boundaries and Structural Defects, Kluwer Academic Publisher, 1989, p. 27.
[8] L. Bourgeois, Rapport CEA-R-5621,1993.
[9] K. Une, I. Tanabe, M. Oguma, J. Nucl. Mater. 150 (1987) 93.
[10] CEA Annual Report 1998.
[11] H.J. Borchardt, J. Inorg. Nucl. Chem. 12 (1959) 113.
[12] H. Kleykamp, J. Nucl. Mater. 206 (1993) 82.
[13] H. Kleykamp, J. Nucl. Mater. 247 (1997) 103.
[14] V.J. Wheeler, I.G. Jones, J. Nucl. Mater. 42 (1972) 117.
[15] Introduction to X-ray Powder Diffractometry, Jenkins & Snyder, Chemical Analysis, vol. 138, Wiley, 1996.
[16] X'Pert Plus, © 1999 Philips Electronics NV.
[17] T.B. Lindemer, T.M. Besmann, J. Nucl. Mater. 130 (1985) 473.
[18] Binary Alloy Phase Diagrams, ASM International.
[19] N.Y. Toker, L.S. Darken, A. Muan, Met. Trans. B 22 (1991) 225.
[20] D.W. Strickler, W.G. Carlson, J. Am. Ceram. Soc. 47 (1964) 122.
[21] L. Vegard, Z. Physik. 17–26 (1921).
[22] R. Alcalá, P. Alonso, V. Orera, H. den Hartog, Phys. Rev. B 32 (1985) 4158.
[23] R.D. Shannon, Acta Cryst. A 32 (1976) 751.